Control-Data Separation across Edge and Cloud for Uplink Communications in C-RAN

Jinkyu Kang*, Osvaldo Simeone†, Joonhyuk Kang‡ and Shlomo Shamai (Shitz)§
*School of Engineering and Applied Sciences, Harvard University, Cambridge, MA, USA
*Department of Electrical Engineering, KAIST, Daejeon, South Korea
†CWCSPR, NJIT, Newark, NJ, USA
§Department of Electrical Engineering, Technion, Haifa, Israel
Email: jkkang@g.harvard.edu

***Abstract*—Fronthaul limitations in terms of capacity and latency motivate the growing interest in the wireless industry for the study of alternative functional splits between cloud and edge nodes in Cloud Radio Access Network (C-RAN). This work contributes to this line of work by investigating the optimal functional split of control and data plane functionalities at the edge nodes and at the Remote Cloud Center (RCC) as a function of the fronthaul latency. The model under study consists of a two-user time-varying uplink channel in which the RCC has global but delayed channel state information (CSI) due to fronthaul latency, while edge nodes have local but timely CSI. Adopting the adaptive sum-rate as the performance criterion, functional splits whereby the control functionality of rate selection and the decoding of the data-plane frames are carried out at either the edge nodes or at the RCC are compared, demonstrating the potential advantages of implementing control functions at the edge.**

***Index Terms*—Cloud-Radio Access Network (C-RAN), fronthaul, control data separation, Fog networking.**

I. Introduction

The evolution of the Cloud Radio Access Network (C-RAN) architecture, as traced from its origin to more recent studies [1], points to a shift from fully centralized baseband processing and control to a more balanced functional split between cloud and edge. In particular, while the basic C-RAN system prescribes the implementation of all functions, excluding possibly analog-to-digital and digital-to-analog conversion, at a cloud processor, more recent proposals enable a flexible number of functionalities to be carried out at the edge nodes. This shift is dictated by the realization that a fully centralized C-RAN system entails significant, and possibly prohibitive, requirements on the fronthaul connections between edge nodes and cloud, see, e.g., [2], [3] and references therein.

The demarcation line between the functionalities to be implemented at the cloud and at the edge is typically drawn to include a given number of physical-layer functions at the edge nodes, such as synchronization, FFT/IFFT and resource demapping [2]. In contrast, reference [4] proposes the application of the *data-control separation architecture* [5] as a guiding principle for the separation of functionalities between edge and cloud with the aim of addressing fronthaul latency limitations.

The work of O. Simeone has been partly supported by the U.S. NSF under grant CCF-1525629. The work of S. Shamai has been supported by the European Union's Horizon 2020 Research And Innovation Programme, grant agreement no. 694630.

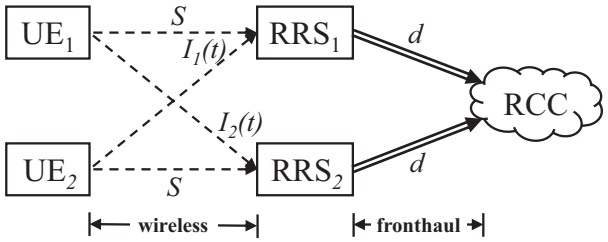

Fig. 1. Uplink of the considered C-RAN system.

In particular, following [6], [7], it is argued therein that the implementation of HARQ control functionalities at the edge can be an enabler for the reduction of transmission latency even in the presence of significant delays on the fronthaul links.

In this work, we study the optimal functional split of control and data plane functionalities at the edge nodes and cloud for uplink communication. We specifically focus on the following functionalities: *(i)* the control plane functionality of the data rate selection, and *(ii)* the data plane functionality of data decoding. We aim at assessing the impact of fronthaul latency on the relative performance of different splits, whereby rate selection and data decoding may be performed separately at either cloud or edge. The model under study consists of a two-user time-varying uplink channel in which the RCC has global but delayed CSI due to fronthaul latency, while the edge nodes have local but timely CSI. Adopting the adaptive sum-rate as the performance criterion (see, e.g., [8]), different functional splits based on the control-data separation architecture are compared through analysis and numerical results.

The rest of the paper is organized as follows. We describe the system model and performance metric in Sec. II. We analyze different control-data functional splits between RCC and RRSs in Sec. III for a Markov channel model with an arbitrary number of states. In Sec. IV, numerical results are presented. Concluding remarks are summarized in Sec. V.

II. System Model and Performance Metric

We consider the uplink of a C-RAN illustrated in Fig. 1, which consists of K access points, referred to as remote radio systems (RRSs), a remote cloud center (RCC), and K active user equipments (UEs). Note that we use the nomenclature of [1] to emphasize that the RRSs may be endowed with more processing capabilities than a standard RRH in a C-RAN

system. We focus here on the scenario with $K = 2$ in order to simplify the arguments, but the analysis can be generalized to larger systems [9]. Each UE i is assigned to a RRS, which is identified as RRS i.

System Model: With the aim of highlighting the impact of interference on the optimal functional split between RRSs and RCC, we model the uplink channels as illustrated in Fig. 1. The signal to noise ratio (SNR) between an UE i and RRS i is denoted as S, and is assumed to be constant over T transmission intervals, while the SNR between an UE j and the RRS $i \neq j$ is denoted as $I_i(t)$, and is assumed to vary across the time index $t = 1, 2, \ldots, T$, which runs over the transmission intervals. Note that the assumption of a constant SNR between UE i and RRS i can be in practice justified in the presence of power control at the UE. The more general scenario with time-varying direct channels is studied in [9]. Furthermore, we assume an ergodic phase fading channel with each transmission interval (see, e.g., [10]), so that the channel matrix between the UEs and the RRSs at any channel use k of the transmission interval $t = 1, 2, \ldots, T$ can be written as

$$\mathbf{H}(t,k) = \begin{bmatrix} \sqrt{S}e^{j\theta_{11}(t,k)} & \sqrt{I_1(t)}e^{j\theta_{12}(t,k)} \\ \sqrt{I_2(t)}e^{j\theta_{21}(t,k)} & \sqrt{S}e^{j\theta_{22}(t,k)} \end{bmatrix}, \quad (1)$$

where the phases $\theta_{ij}(t,k)$ are uniformly distributed in the interval $[0, 2\pi]$, mutually independent, and vary in an ergodic manner over the channel use index k within each transmission interval t. Note that an ergodic phase fading model may be appropriate on wireless channels where its phase may vary rapidly over all possible states due to small scale mobility and the phase information $\theta_{ji}(t,k)$ is available at the receiver [10], [11].

Each RRS i is connected to the RCC via a fronthaul link with a delay of d transmission intervals. As an example, fronthaul transport latency is reported to be around 0.25 ms in [12] for single-hop fronthaul links and can amount to multiple milliseconds in the presence of multihop fronthauling, while fronthaul-related processing at the RCC can take fractions to a few milliseconds [13]. As a result, for transmission intervals of, say $0.5-1$ ms, d can be as large as $3-5$. Due to the fronthaul delay d, the RCC has global but delayed CSI, namely $I_i(t-d)$ for $i \in \{1, 2\}$. In contrast, each RRS i at time t has local but instantaneous CSI about the cross-channel $I_i(t)$. This information can be obtained, e.g., by means of uplink training in a Time Division Duplex system.

For tractability, we assume at first that the SNR $I_i(t)$ on the cross-channel between UE j and RRS i with $i \neq j$ is in two states, namely I_L and I_H with $I_H \geq I_L$. Moreover, the time-varying interference state is governed by the Markov Chain in Fig. 2, with transition probabilities $p = \Pr[I_i(t+1) = I_H | I_i(t) = I_L]$ and $q = \Pr[I_i(t+1) = I_L | I_i(t) = I_H]$. The channels $I_i(t)$ for $i = 1, 2$ are mutually independent. Based on the definitions above, the probability that the interference state y changes the state x for $x, y \in \{I_L, I_H\}$ after d transmission intervals can be written as

$$\Pr\left[I_i(t) = x | I_i(t-d) = y\right] = \beta^{x|y}(d), \quad (2)$$

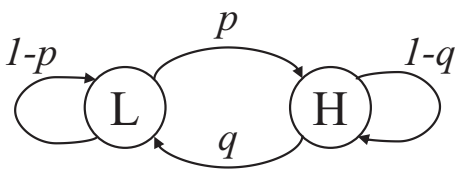

Fig. 2. Markov model for the cross-channel processes $I_1(t)$ and $I_2(t)$.

where the probability $\beta^{x|y}(d)$ is obtained as the (x, y) entry of the matrix $\mathbf{T}^d$, with

$$\mathbf{T} = \begin{bmatrix} 1-p & p \\ q & 1-q \end{bmatrix} \quad (3)$$

being the transition matrix of the Markov chain in Fig. 2. Moreover, the stationary probabilities for the "low" and "high" states are obtained as

$$\pi_L = \frac{q}{p+q} \quad \text{and} \quad \pi_H = \frac{p}{p+q}, \quad (4)$$

respectively. A memory parameter μ can be also defined as $\mu \triangleq 1 - p - q$ and is the second eigenvalue of the transition matrix $\mathbf{T}$. Accordingly, $\mu = 1$ represents a static interference process and $\mu = 0$ represents an i.i.d. interference process. The memory parameter μ can be related to the coherence time of the channel (see Sec. IV). A more general Markovian model for the cross-channels, as well as for the direct channels, is studied in [9].

RCC-RRS Functional Splits: Our focus is on the optimization of the functional split between RCC and RRSs, that is, between cloud and edge. Specifically, we consider three different control-data functional splits, as described below; *(i) Decentralized control-decentralized data* (DC-DD) functional split amounts to the most conventional cellular implementation in which control and data plane functionalities are carried out at the RRSs, that is, at the edge; *(ii) Centralized control-centralized data* (CC-CD) functional split corresponds to the standard C-RAN implementation in which the RCC carries out both control and data processing; *(iii) Decentralized control-centralized data* (DC-CD) functional split is this hybrid implementation in which each RRS individually performs decentralized control and the RCC instead performs centralized joint data decoding.

Performance Metric: To compare different functional splits, we will use the performance metric of the *adaptive sum-rate* (with no power control) used in [8] and references therein. This is defined as the average sum-rate that can be achieved while guaranteeing no outage in each transmission slot, where the average is taken here with respect to the steady-state distribution (4) of the random channel gains $\{I_1(t), I_2(t)\}$. To be more precise, in each transmission interval, transmission rates R_1 for user 1 and R_2 for user 2 are chosen by the RCC or by the RRSs, depending on the functional splits, so that no outage occurs. The adaptive sum-rate is the average of the sum rates $R_1 + R_2$. We will also consider, as discussed below, a generalized metric, termed *adaptive outage sum-rate*, in which a (small) outage probability ϵ is allowed, where an outage event is caused by the imperfect knowledge of the CSI.

III. Analysis of the Control-Data Functional Splits

In this section, we analyze the performance in terms of the adaptive sum-rates of the mentioned control-data functional splits between RCC and RRSs in the presence of the fronthaul transmission delay d. Throughout, we define C_{xy} as

$$C_{xy} \triangleq \mathbb{E}[\log_2 \det(\mathbf{I} + \mathbf{H}_{xy}\mathbf{H}_{xy}^{\dagger})], \tag{5}$$

for $x, y \in \{L, H\}$, where $\mathbf{H}_{xy} = [\sqrt{S}e^{j\theta_{11}}\ \sqrt{I_x}e^{j\theta_{12}}; \sqrt{I_y}e^{j\theta_{21}}\ \sqrt{S}e^{j\theta_{22}}]$ and the expectation is taken over the random phases $\boldsymbol{\theta} = [\theta_{11}, \theta_{12}, \theta_{21}, \theta_{22}]$ which are mutually independent and uniformly distributed in the interval $[0, 2\pi]$. Note that this is the maximum achievable sum-rate in a time-slot with $I_1(t) = I_x$ and $I_2(t) = I_y$ if joint data decoding is performed at the RCC (see, e.g., [14, Ch. 4]). We will also use the notation $C_{I_1 I_2}$ for C_{xy} when $I_1 = I_x$ and $I_2 = I_y$. We also observe that $C_{LH} = C_{HL}$.

A. Decentralized Control - Decentralized Data (DC-DD)

Here, we study the conventional cellular implementation based on DC-DD. Accordingly, each RRS i selects the transmission rate R_i for the user i in its cell based on the available current CSI $I_i(t)$ and performs local data decoding. We further assume the standard approach of treating interference from the out-of-cell user as noise for local decoding.

Based on the mentioned assumptions, the rate for each user can be adapted at each RRS based on the CSI $I_i(t) = I_x$ by choosing the transmission rate $R_i = R_x \triangleq \log_2(1 + S/(1 + I_x))$. This choice guarantees no outage. The resulting maximum adaptive sum-rate R^{DC-DD} is summarized in the following lemma. Note that this rate does not depend on the fronthaul delay d, which does not affect the performance of DC-DD.

Lemma 1: With DC-DD, the maximum adaptive sum-rate is given by

$$R^{DC-DD} = 2\pi_L^2 R_L + 2\pi_L \pi_H (R_L + R_H) + 2\pi_H^2 R_H. \tag{6}$$

B. Decentralized Control - Centralized Data (DC-CD)

With DC-CD, the transmission rate R_i for user i is selected by each RRS i based on the available current CSI $I_i(t)$ as for DC-DD, while the RCC performs centralized joint data decoding on behalf of the RRSs. The set of achievable rate pairs (R_1, R_2) with joint decoding at the RCC is given by the capacity region $\mathcal{C}_{I_1(t)I_2(t)}$ of the ergodic multiple access channel between the two users at the two RRSs. Using standard results in network information theory (see, e.g., [14, Ch. 4]), we have

$$\mathcal{C}_{I_1(t)I_2(t)} = \left\{ (R_1, R_2) \;\middle|\; \begin{array}{c} R_1 \le \log_2(1 + S + I_2(t)) \\ R_2 \le \log_2(1 + S + I_1(t)) \\ R_1 + R_2 \le C_{I_1(t)I_2(t)} \end{array} \right\}. \tag{7}$$

The capacity regions $\mathcal{C}_{LL}$, $\mathcal{C}_{LH}$, $\mathcal{C}_{HL}$, $\mathcal{C}_{HH}$ are illustrated in Fig. 3.

We define as R_L and R_H the rates selected by each RRS i when $I_i(t) = I_L$ and $I_i(t) = I_H$, respectively. The outage probability is the probability that the rate pair $(R_{I_1(t)}, R_{I_2(t)})$ does not belong to the capacity region $\mathcal{C}_{I_1(t)I_2(t)}$. The next proposition provides the maximum adaptive sum-rate for DC-CD based on an optimized choice of the rates R_L and R_H. Specifically, it shows that the optimal rate pairs (R_L, R_L), (R_L, R_H), (R_H, R_L) and (R_H, R_H) are given by the points a, b, c and d, respectively, in Fig. 3.

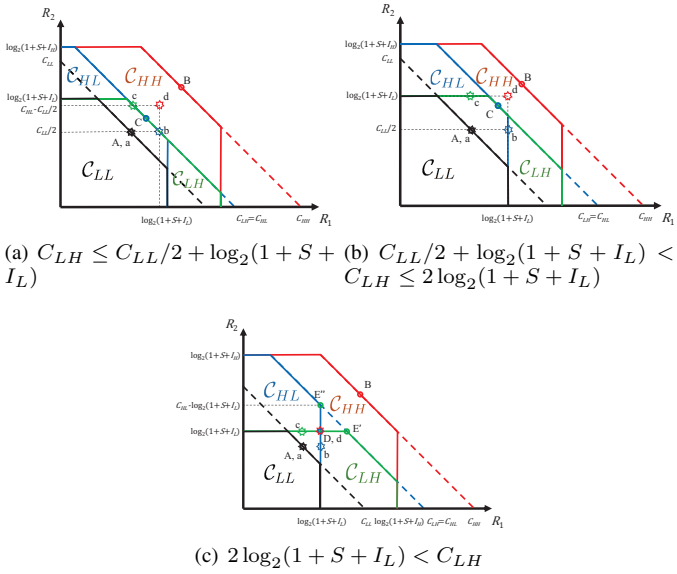

(a) $C_{LH} \le C_{LL}/2 + \log_2(1 + S + I_L)$ (b) $C_{LL}/2 + \log_2(1 + S + I_L) < C_{LH} \le 2\log_2(1 + S + I_L)$

(c) $2\log_2(1 + S + I_L) < C_{LH}$

Fig. 3. Capacity regions $\mathcal{C}_{xy}$ in (7) when the interference realizations are $I_1 = I_x$ and $I_2 = I_y$ if (a) $C_{LH} \le C_{LL}/2 + \log_2(1 + S + I_L)$; (b) $C_{LL}/2 + \log_2(1 + S + I_L) < C_{LH} \le 2\log_2(1 + S + I_L)$; and (c) $2\log_2(1 + S + I_L) < C_{LH}$. The points a, b, c, and d indicate the four rate pairs (R_x, R_y) selected by the DC-CD scheme in Sec. III-B and the points A, B, C, D, E, and E' denote the rates selected by the RCC in the CC-CD scheme discussed in Sec. III-C.

Proposition 1: With DC-CD, the maximum adaptive sum-rate R^{DC-CD} is given as

$$R^{DC-CD} = 2\pi_L^2 R_L + 2\pi_L \pi_H (R_L + R_H) + 2\pi_H^2 R_H, \tag{8}$$

where R_L is given as

$$R_L = \begin{cases} C_{LL}/2 & \text{if } C_{LH} > C_{LL}/2 + \log_2(1+S+I_L), \\ C_{LL}/2 & \text{if } C_{LH} \le C_{LL}/2 + \log_2(1+S+I_L) \text{ and } \pi_L^2 > \pi_H^2, \\ C_{LH} - \log_2(1 + S + I_L) & \text{otherwise,} \end{cases} \tag{9}$$

and R_H is given as

$$R_H = \begin{cases} \log_2(1 + S + I_L) & \text{if } C_{LH} > C_{LL}/2 + \log_2(1+S+I_L), \\ C_{LH} - C_{LL}/2 & \text{if } C_{LH} \le C_{LL}/2 + \log_2(1+S+I_L) \text{ and } \pi_L^2 > \pi_H^2, \\ \log_2(1 + S + I_L) & \text{otherwise.} \end{cases} \tag{10}$$

Proof: The details are available in [9, Proposition 1]. ■

C. Centralized Control - Centralized Data (CC-CD)

With the C-RAN mode of CC-CD processing, at any transmission interval t, the RCC performs rate adaptation in a centralized manner based on the available delayed CSI, namely $\{I_1(t-d), I_2(t-d)\}$. Furthermore, the RCC performs centralized joint data decoding on behalf of the connected RRSs. Due to joint decoding, an outage occurs at time t if the rate pair $(R_{1,xy}, R_{2,xy})$ selected by the RCC when the delayed CSI is $I_1(t-d) = I_x$ and $I_2(t-d) = I_y$ is outside the capacity region $\mathcal{C}_{I_1(t)I_2(t)}$ in (7). Accordingly, the outage probability P_{xy}^{out} in a time slot t for which the CSI available

at the scheduler is $I_1(t-d)=I_x$ and $I_2(t-d)=I_y$ can be computed as

$$P_{xy}^{out}=\Pr\left[(R_{1,xy},R_{2,xy})\notin\mathcal{C}_{I_1(t)I_2(t)}|I_1(t-d)=I_x,I_2(t-d)=I_y\right]. \quad (11)$$

For reference, we first observe the case of no fronthaul delay, i.e., $d=0$, the RCC has perfect CSI $I_i(t)$ for all $i\in\{1,2\}$. Therefore, the RCC can adapt the transmission rates to the current CSI to achieve the maximum sum-rate $C_{I_1(t)I_2(t)}$ due to joint decoding at the RCC. The resulting adaptive sum-rate is given as

$$R_{d=0}^{CC-CD}=\pi_L^2C_{LL}+2\pi_L\pi_HC_{LH}+\pi_H^2C_{HH}. \quad (12)$$

This follows since, when $I_1(t)=I_x$ and $I_2(t)=I_y$, the RCC can select the rates $R_{1,xy}$ and $R_{2,xy}$ such that the selected rates are inside the capacity region $\mathcal{C}_{xy}$ and $R_{1,xy}+R_{2,xy}=C_{xy}$ (see Fig. 3).

In contrast to the case with no fronthaul delay, if the fronthaul link has delay d, the RCC has delayed CSI, namely $\{I_1(t-d),I_2(t-d)\}$, and is hence not informed about the current capacity region $\mathcal{C}_{I_1(t)I_2(t)}$ in (7). An outage event can thus be generally avoided only if transmitting always at the minimum sum-rate C_{LL}, since the latter yields rate pairs that are within the capacity region in all other states. Therefore, with $d>0$, the adaptive sum-rate of CC-CD is given by $R_d^{CC-CD}=C_{LL}$.

Based on the discussion above, CC-CD is outperformed by DC-CD when $d>0$ in terms of adaptive sum-rate. To enable additional insights into the performance of CC-CD, we then consider a generalized performance metric, termed *adaptive outage sum-rate*, that allows for an outage probability (11) no larger than ϵ. We note that this definition is sensible for CC-CD since outage event can occur in this case due to the, typically small, uncertainty about the CSI at the RCC in the practical case when d is not large. This is not the case with DC in which each RRS has no CSI about the cross-channel relative to the other RRS. To formulate the resulting adaptive outage sum-rate, we define the probabilities $P_{xy}^{HH}=\beta^{H|x}(d)\beta^{H|y}(d)$, $P_{xy}^{LH}=\beta^{L|x}(d)\beta^{H|y}(d)$, $P_{xy}^{HL}=\beta^{H|x}(d)\beta^{L|y}(d)$, and $P_{xy}^{LL}=\beta^{L|x}(d)\beta^{L|y}(d)$, where the notation $P_{xy}^{x'y'}$ indicates the probability of transitioning from delayed states $\{I_1(t-d)=I_x,I_2(t-d)=I_y\}$ to current states $\{I_1(t)=I_{x'},I_2(t)=I_{y'}\}$. The next proposition provides an achievable outage adaptive sum-rate.

Proposition 2: With CC-CD, the outage adaptive sum-rate $R_d^{CC-CD}(\epsilon)$ is achievable with outage probability ϵ, where

$$R_d^{CC-CD}(\epsilon)=\pi_L^2R_{LL}+2\pi_L\pi_HR_{LH}+\pi_H^2R_{HH}, \quad (13)$$

with R_{xy} being defined as

$$R_{xy}=\begin{cases}C_{LL} & \text{if } \epsilon\le P_{xy}^{LL},\\ C_{LH} & \text{if } P_{xy}^{LL}<\epsilon\le 1-P_{xy}^{HH},\\ C_{HH} & \text{if } 1-P_{xy}^{HH}<\epsilon\le 1,\end{cases} \quad (14)$$

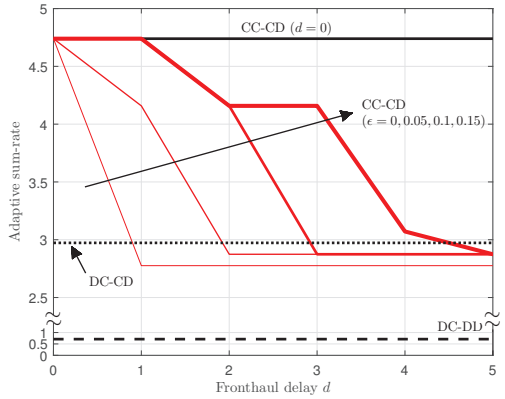

Fig. 4. Adaptive sum-rate vs. fronthaul delay d under two-state Markov model for the cross-channels ($N_S=N_I=2$, $SNR=0$ dB, $SIR_H=-10$ dB, $SIR_L=0$ dB, $\mu=0.9$, and $p=q=(1-\mu)/2$).

if $C_{LH}\le 2\log_2(1+S+I_L)$, and as

$$R_{xy}=\begin{cases}C_{LL} & \text{if } \epsilon\le P_{xy}^{LL},\\ 2\log_2(1+S+I_L) & \text{if } P_{xy}^{LL}<\epsilon\le \widetilde{P}_{xy},\\ C_{LH} & \text{if } \widetilde{P}_{xy}<\epsilon\le 1-P_{xy}^{HH},\\ C_{HH} & \text{if } 1-P_{xy}^{HH}<\epsilon\le 1,\end{cases} \quad (15)$$

if $C_{LH}>2\log_2(1+S+I_L)$, with $\widetilde{P}_{xy}=\min(P_{xy}^{LH},P_{xy}^{HL})+P_{xy}^{LL}$.

Proof: The RCC chooses the rates $R_{1,xy}$ and $R_{2,xy}$ when $I_1(t-d)=I_x$ and $I_2(t-d)=I_y$ in such a way that the probability that the chosen rates are outside the capacity region $\mathcal{C}_{I_1(t)I_2(t)}$ in (7) is less than ϵ. Specifically, referring to Fig. 3 for an illustration, the RCC selects the rate pair $(R_{1,xy},R_{2,xy})$ at the point A if $\epsilon\le P_{xy}^{LL}$; at the point B if $1-P_{xy}^{HH}<\epsilon\le 1$; at the point C if $P_{xy}^{LL}<\epsilon\le 1-P_{xy}^{HH}$ and $C_{LH}\le 2\log_2(1+S+I_L)$; at the point D if $P_{xy}^{LL}<\epsilon\le\widetilde{P}_{xy}$ and $C_{LH}>2\log_2(1+S+I_L)$; and at either the point E′ or E″ if $\widetilde{P}_{xy}<\epsilon\le 1-P_{xy}^{HH}$ and $C_{LH}>2\log_2(1+S+I_L)$, where the first rate pair is selected when $P_{xy}^{HL}+P_{xy}^{LL}<P_{xy}^{LH}+P_{xy}^{LL}$ and the other pair otherwise.

The proof that the outage probability (11) with these choices is no larger than ϵ is available in [9, Appendix 1]. ■

IV. Numerical Results

In this section, we evaluate the performance of the considered splits of control and data functions between cloud and edge in terms of the adaptive (outage) sum-rate as a function of key system parameters such as fronthaul delay and channel variability. We start by considering the case studied in Sec. III, in which the direct channels are fixed, due to power control, while the cross-channels vary according to the two-state Markov chain in Fig. 2. Under this model, in Fig. 4 and Fig. 5, we set the SNR of the desired signal as $SNR=S/N_0=0$ dB with noise power $N_0=1$; and we assume that the SIR is $SIR_H=S/I_H=-10$ dB when the cross-channel is in the high state I_H, while it equals $SIR_L=S/I_L=0$ dB when the cross-channel is in the low state I_L. Moreover, we parameterize the transition probabilities p and q as $p=q=(1-\mu)/2$, with μ being the memory parameter discussed in Sec. II.

For the mentioned conditions, Fig. 4 shows the adaptive sum-rate as function of the fronthaul delay d when the memory

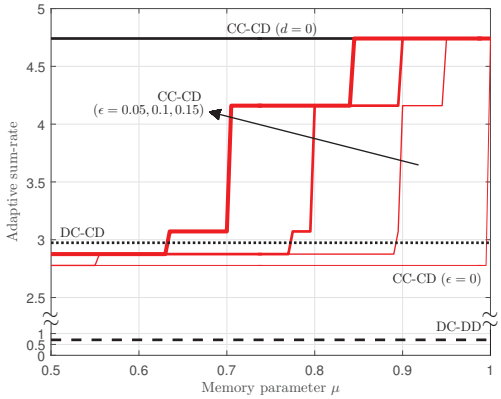

Fig. 5. Adaptive sum-rate vs. memory parameter μ under two-state Markov model for the cross-channels ($N_S = N_I = 2$, $SNR = 0$ dB, $SIR_H = -10$ dB, $SIR_L = 0$dB, $d = 1$ and $p = q = (1-\mu)/2$).

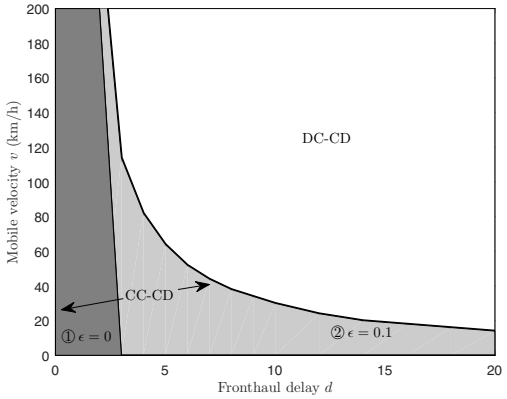

Fig. 6. Regions of the plane (d, v) in which DC-CD or CC-CD yield a larger adaptive sum-rate when allowing an outage of $\epsilon = 0$ (region ①) and $\epsilon = 0.1$ (region ②) under the finite-state Markov model [15] for both signal and interference processes ($N_S = N_I = 6$, $\gamma_S = -5$ dB, and $\gamma_I = 5$ dB).

parameter is $\mu = 0.9$. With this choice, the average coherence time is $1/p = 1/q = 20$ transmission intervals. For reference, under Clarke's model, when the carrier frequency is $c/\lambda = 1$ GHz, where $c = 3 \times 10^8$ m/s and λ is the wavelength, and the transmission interval is 0.5 ms, using the approximate expression for the coherence time $0.423\,\lambda/v$, this corresponds to a velocity $v \approx 46$ km/h. From the figure, we first observe that, as expected, the *centralized data decoding* performed by DC-CD strictly improves over the decentralized decoding of DC-DD, irrespective of the fronthaul delay d, which does not affect the performance of either scheme. In contrast, the *centralized control* carried out by CC-CD is only able to enhance the sum-rate when the fronthaul latency is sufficiently small and the system allows for a non-zero outage. For example, for an outage level $\epsilon = 0.05$, CC-CD improves over DC-CD only as long as the fronthaul latency is no larger than two transmission intervals, i.e., $d < 2$.

The impact of the memory parameter μ is studied in Fig. 5, where the adaptive sum-rate is plotted versus μ with a fronthaul delay $d = 1$. We only show the range $\mu > 0.5$ since, for $\mu < 0.5$, the sum-rates do not change significantly as compared to $\mu = 0.5$. We note that, for Clarke's model with the parameters discussed above, the range $[0.5, 1]$ for μ corresponds approximately to interval of velocities $[0, 230]$ (km/h). In keeping with the discussion above, CC-CD is seen to outperform DC-CD for μ sufficiently large. For example, with $\epsilon = 0.1$ at $\mu = 0.9$, CC-CD provides a rate gain over the decentralized schemes. Overall, this discussion points to a conclusion for the problem of scheduling in a multi-hop network (see Sec. I): *Centralized control based on global but delayed CSI can yield a degraded performance as compared to decentralized control based on local but timely CSI*.

We now turn to consider the more general case detailed in [9] in which both direct channel and cross-channel vary according to Markov chains with $N_S = N_I > 2$ states. Specifically, we adopt the equal-probability method proposed in [15] to approximate Clarke's model with a finite-state Markov chain (see in detail [9]). In order to obtain further insight into the operating requires in which different functional splits are to be preferred, Fig. 6 shows the regions of the plane with coordinates given by the fronthaul delay d and mobile velocity v in which each scheme offers the best adaptive sum-rate. The DC-CD scheme is seen to be advantageous in the area above the uppermost solid line, while CC-CD with $\epsilon \leq 0.1$ is to be preferred in the complementary regime below this line. In particular, in the region ① CC-CD outperforms DC-CD, and hence also DC-DD, even when allowing for no outage, while in the region ② CC-CD outperforms DC-CD for $\epsilon = 0.1$. The uppermost boundary lines for each region hence provide the maximum fronthaul delay d that can be tolerated by the CC-CD scheme for a given value of v while still yielding gains as compared to DC-CD scheme when $\epsilon = 0$ or $\epsilon = 0.1$.

V. Conclusions

In this paper, we have analyzed the relative merits of alternative functional splits for C-RAN based on control-data separation. Our results show that moving the control functionality of rate selection at the edge while performing joint data decoding at the cloud yields potentially significant gains. This conclusion demonstrates the value of "fog" networking solutions in the evolution of C-RAN.

References

[1] J. Huang and Y. Yuan, "White paper of next generation fronthaul interface," *[Online]. Available: labs.chinamobile.com/cran*, ver. 1.0, China mobile Research Institute, Jun. 2015.

[2] D. Wubben, P. Rost, J. Bartelt, M. Lalam, V. Savin, M. Gorgoglione, A. Dekorsy, and G. Fettweis, "Benefits and impact of cloud computing on 5G signal processing: Flexible centralization through cloud-RAN," *IEEE Sig. Proc. Mag.*, vol. 31, no. 6, pp. 35–44, Nov. 2014.

[3] O. Simeone, A. Maeder, M. Peng, O. Sahin, and W. Yu, "Cloud radio access network: Virtualizing wireless access for dense heterogeneous networks," *Journal of Communications and Networks*, vol. 18, no. 2, pp. 135–149, Apr 2016.

[4] S. Khalili and O. Simeone, "Uplink HARQ for cloud ran via separation of control and data planes," to appear in *IEEE Trans. Veh. Techn.*, 2016.

[5] A. Mohamed, O. Onireti, M. Imran, A. Imran, and R. Tafazolli, "Control-data separation architecture for cellular radio access networks: A survey and outlook," *IEEE Communications Surveys and Tutorials*, vol. 18, no. 1, pp. 446–465, Jun. 2015.

[6] U. Dotsch, M. Doll, H. P. Mayer, F. Schaich, J. Segel, and P. Sehier, "Quantitative analysis of split base station processing and determination of advantageous architectures for LTE," *Bell Labs Technical Journal*, vol. 18, no. 1, pp. 105–128, Jun. 2013.

[7] P. Rost and A. Prasad, "Opportunistic hybrid ARQ: Enabler of centralized-RAN over nonideal backhaul," *IEEE Wireless Comm. Lett.*, vol. 3, no. 5, pp. 481–484, Jul. 2014.

[8] S. Sreekumar, B. Dey, and S. Pillai, "Distributed rate adaptation and power control in fading multiple access channels," *IEEE Trans. Info. Th.*, vol. 61, no. 10, pp. 5504–5524, Oct. 2015.

[9] J. Kang, O. Simeone, J. Kang, and S. Shamai, "Control-data separation across edge and cloud for uplink communications in C-RAN," *arXiv:1606.09137*.

[10] G. Kramer, M. Gastpar, and P. Gupta, "Cooperative strategies and capacity theorems for relay networks," *IEEE Trans. Info. Th.*, vol. 51, no. 9, pp. 3037–3063, Sep. 2005.

[11] S. A. Jafar, "The ergodic capacity of phase-fading interference networks," *IEEE Trans. Info. Th.*, vol. 57, no. 12, pp. 7685–7694, Dec. 2011.

[12] NGMN Alliance, "Further study on critical C-RAN technologies," *[Online] Available: https://www.ngmn.org*, Mar. 2015.

[13] N. Nikaein, "Processing radio access network functions in the cloud: Critical issues and modeling," *in Proc. of Int. Workshop on Mobile Cloud Computing and Services*, pp. 36–42, Paris, France, Sep. 2015.

[14] A. E. Gamal and Y.-H. Kim, *Network Information Theory*. Cambridge University Press, 2011.

[15] H. S. Wang and N. Moayeri, "Finite-state Markov channel-a useful model for radio communication channels," *IEEE Trans. on Veh. Technol.*, vol. 44, no. 1, pp. 163 –171, Feb. 1995.